Banner appropriate to article type will appear here in typeset article

# Preventing sinking of a disk by leveraging the Parametric Hydraulic Jump phenomenon

**Jan Turczynowicz[12], Radost Waszkiewicz[12], and Łukasz Gładczuk[13]**†

[1]Fenix Science Club, Aleja Stanów Zjednoczonych 24, 03-964 Warsaw

[2]Institute of Theoretical Physics, Faculty of Physics,
University of Warsaw, L. Pasteura 5, 02-093 Warsaw, Poland

[3]Department of Physics, Clarendon Laboratory,
University of Oxford, Oxford OX1 3PU, United Kingdom

Although it is commonly expected that a metal disk placed on the surface of water will sink, our investigation has revealed a surprising phenomenon: a vertical jet directed onto the disk from above can allow it to remain afloat. This result defies intuition, as one would assume that the force of the jet's impact would cause the disk to sink. We have discovered that this phenomenon occurs as a result of water displacement from the top of the disk caused by the impacting jet, operating through a mechanism similar to a classical hydraulic jump. This displacement generates a difference in hydrostatic pressures, resulting in an upward buoyancy force capable of balancing the force of gravity. In contrast to the classical case, here the jump radius is fixed by the geometric parameters of a disk, a phenomenon we refer to as the *parametric hydraulic jump*. To further explore this effect, we have presented a theoretical model based on scaling laws, which provides the conditions required for the disk to float. The dimensionless scaling constant's value was determined through an independent experiment. Finally, we conducted experiments on the disk's floating and sinking, which showed a good match with the proposed theory.

## 1. Introduction

Placing a thin metal disk on the surface of water and directing a vertical water jet onto the disk reveals an unusual phenomenon. Despite the disk being denser than water, in some cases, the weight of water displaced from the surface of the disk is sufficient for the buoyancy force to balance both the impact force of the jet and the weight of the disk. This balance allows the disk to remain afloat.

To understand the necessary conditions for this phenomenon to occur, it is essential to study the water flow dynamics on the upper surface of the disk. Due to the cylindrical symmetry

† Email address for correspondence: lukasz@fenix.club

of the flow and the very thin layer of fast-moving liquid, this process is reminiscent of the classical hydraulic jump problem.

The hydraulic jump has been a research topic at least since works of Rayleigh (1914). Today, even with different variants of the geometry studied (Ivanova & Gavrilyuk 2019; Teymourtash & Mokhlesi 2015; Wang & Khayat 2019, 2018), details of the phenomenon still remain a debated issue cf. (Bhagat *et al.* 2018; Duchesne & Limat 2022). Qualitatively, when a jet hits a plate, a region of higher pressure at the centre of the disk necessarily appears. In the region very close to the centre of the disk, where the boundary layer flow is not yet developed (Baayoun *et al.* 2022), flow pattern is similar to the one of an inviscid flow where high pressure at the centre accelerates the liquid outwards. As the fluid moves further from the centre a combination of outward acceleration and increased circumference leads to rapid decrease of the film thickness $h$ (with $h \sim 1/r^2$, where $r$ denotes the distance from the centre of the disk; Landau & Lifshitz 1987, 10 problem 5.1) until the film is so thin that the viscous forces become significant. This thin layer proves to be unstable and an abrupt transition to a subcritical, thicker layer, happens at the distance $R_J$ from the centre of the system. Works of Watson (1964) and Bohr *et al.* (1993) based on boundary layer theories show an experimentally validated scaling of $R_J$ for a jet of volumetric flux $Q$, kinematic viscosity $\nu$ and density $\rho$ to be

$$R_J \sim Q^{5/8} \nu^{-3/8} g^{-1/8}, \tag{1.1}$$

where $g$ is the gravitational acceleration. A recent work of Bhagat *et al.* (2018) presented a different, also experimentally validated, scaling law

$$R_J \sim Q^{3/4} \rho^{1/4} \nu^{-1/4} \sigma^{-1/4}, \tag{1.2}$$

where $\sigma$ is the surface tension coefficient, claiming $g$ has no influence on the location of the hydraulic jump. This was later contested in (Duchesne *et al.* 2019) and (Bohr & Scheichl 2021).

Both approaches indicate that the radius of the hydraulic jump increases with an increase in the volumetric flux ($Q$). This relationship holds true for the investigated finite disk only when $R_J \lesssim R_{disk}$. However, when $Q$ reaches values that would cause the radius of the jump to exceed the radius of the disk, the jump position becomes fixed to the radius of the disk and the above expressions are no longer valid.

Experimental investigations revealed that, as the disk's submersion depth increases, a transition between two distinct regimes occurs (Figure 1b, c). We refer to the two regimes as type I and type IIa jumps, following the nomenclature of Ellegaard *et al.* (1996) and subsequent works of Yokoi & Xiao (1999); Wang & Khayat (2019); Teymourtash & Mokhlesi (2015); Bush *et al.* (2006). In the type I jump the water continues to flow away from the disk after crossing the jump boundary. However, with greater submersion of the disk, the water encounters a larger mass of non-moving water outside the disk boundaries, significantly slowing down. This change in dynamics causes water re-circulation, resulting in water flowing back onto the top of the disk (type IIa jump).

We noticed that the type of jump coincides with the ability of the disk to float. The disk would float only when a type I jump, similar to the one depicted in Figure 1b, was very pronounced.

## 2. Parametric hydraulic jump

As the first step of our investigation, we focused on the flow dynamics, independent of the floating dynamics. By fixing the disk to the bottom of the liquid container with a variable-
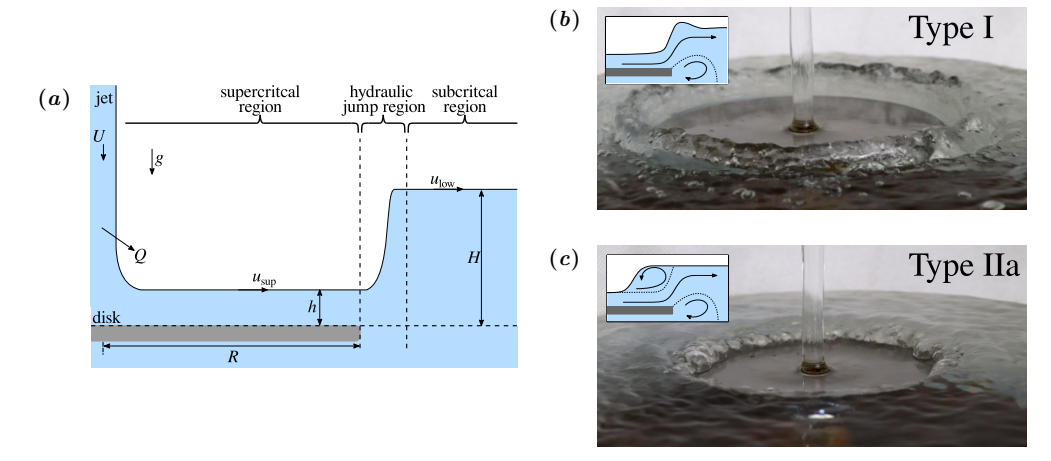
Figure 1: Sketch (a) shows the flow pattern on the top of the disk. Jet, characterised by flux $Q$ and cross-sectionally averaged velocity $U$, impacts the disk creating a supercritical layer of thickness $h$ and velocity $u_{sup}$. Near the disk's edge, a parametric hydraulic jump occurs, leading to a rapid increase in the liquid layer thickness to $H$ and a reduction in liquid velocity to $u_{low}$. Depending on the value of $H$ two types of jumps are observed. At $H = 2.5$ mm a type I jump (b) occurs – where the entire disk is visible with a characteristic high wave formed close to its edge. For a larger value of $H = 5.5$ mm a type IIa jump (c) is observed – the edge of the disk is covered by the water, and water close to the jump edge is moving *towards* the centre of the disk. The experiments shown in photos (b) and (c) used a disk with a radius of $R = 6$ cm, a jet flux of $Q = 104$ ml/s, and a velocity of $U = 1.7$ m/s.
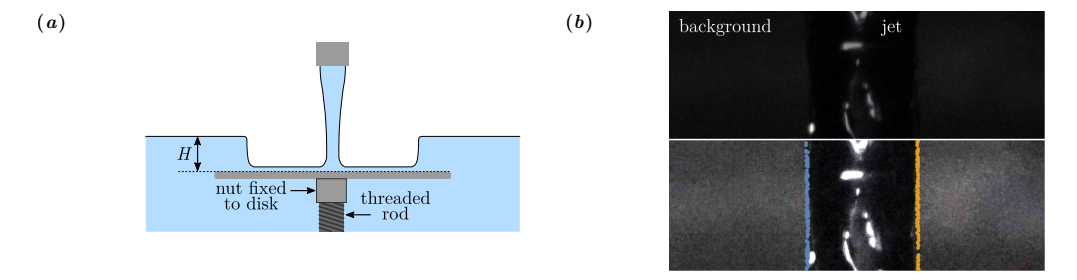


Figure 2: Sketch (a) illustrates the experimental setup utilised to determine the critical depth of the regime transition, $h_{crit}$. The disk's bottom was attached to a nut that could be moved along a vertical, threaded rod, affixed to the bottom of a large vessel. This arrangement enabled variation in the disk's submersion depth ($H$). The radius of the jet ($r$) was measured by taking a side photo of the jet and performing image analysis, as shown in (b). The top image displays the original photograph before analysis, while the bottom image, with enhanced contrast for better readability, shows the detected jet boundaries.

height pillar, we precisely controlled the submersion depth of the disk. Changing this depth reproduced the two hydraulic jump regime patterns, type I and type IIa. As shown in the inset of the Figure 1b, when the submersion depth was small, water on surface flowed outward. With an increase in the submersion depth, past a critical value $h_{crit}$, a region of recirculation appeared near the edge of the disk (Figure 1c), causing the water to flow back onto the top surface of the disk.

### 2.1. *Scaling analysis*

Hydraulic jumps are frequently modelled using scaling laws (e.g. Bhagat *et al.* (2018)). In line with these methodologies, we develop a model for the critical disk submersion depth
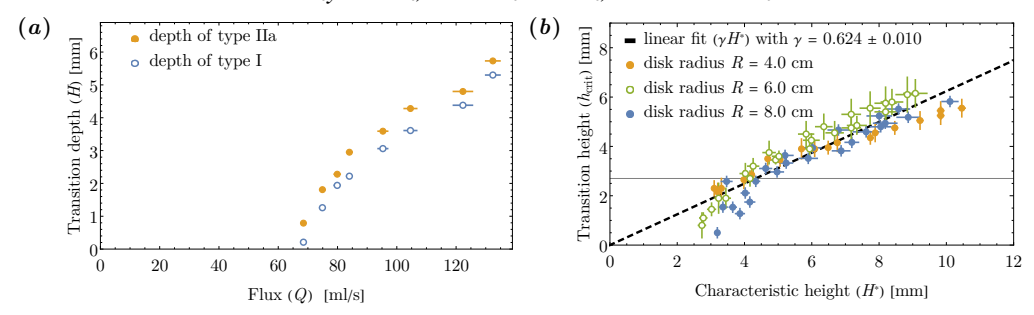
Figure 3: The measurement series (a) was obtained by varying the jet flux while maintaining a constant nozzle height, resulting in a variable but measured jet radius. For each level of jet flux, the disk ($R = 6$ cm) was slowly moved vertically to determine the boundary of each flow regime. The orange and blue symbols in the graph represent observations of type I and type IIa flow patterns, respectively, observed around the disk. A master-curve (b) was constructed from multiple measurement series by calculating $h_{crit}$ and $H^*$. In the graph, various symbols denote disks with different radii. The horizontal dashed line marks the capillary length of 2.7 mm. Measuring the flow pattern below this capillary length presented notable challenges. A linear fit, shown as a solid line, was applied to all data where the transition depth exceeded this capillary length.

$h_{crit}$ which marks the transition between type I and type IIa hydraulic jump. In our specific scenario, illustrated in Figure 1a, the jet impacts the centre of the disk with a constant flux $Q$. This impact generates a supercritical flow layer atop the disk, characterised by a height $h$ and a radial surface velocity $u_{sup}$. At the disk's periphery (radius $R$), this supercritical layer interacts with the adjacent water, which, due to its significantly larger volume, possesses greater inertia. Consequently, the fluid's velocity near the edge reduces to a subcritical level, $u_{low}$. This deceleration results in the elevation of the water's surface level to a height $H$, indicating a conversion of the fluid's kinetic energy into an increase in potential energy.

Assuming that the viscous drag balances the radial flow (Bhagat *et al.* 2018; Landau & Lifshitz 1987, ch. IV), leads to the following scaling:

$$\frac{u_{sup}}{R} \sim \frac{\nu}{h^2}. \tag{2.1}$$

Guided by our experimental observations, we assume that $u_{sup} \gg u_{low}$ and that $h \ll H$. The flow height ($h$) is estimated by applying the supercritical flow model described by Watson (1964), yielding typical values around $h \sim 0.1$ mm and $H \sim 5$ mm. The ratio $u_{low}/u_{sup}$ can be estimated using the conservation of mass, which suggests a typical value on the order of $10^{-2}$.

Considering the transition between the supercritical and the subcritical region, one can neglect the hydrostatic pressure influence before the jump and the kinetic energy after it. Thus, the energy conservation for a thin slice of the liquid yields

$$\frac{1}{2}\rho u_{sup}^2 h \sim \frac{1}{2}\rho g H^2. \tag{2.2}$$

As the continuity implies $Q = 2\pi u_{sup} R h$, the maximal value of $H$ which can be supported at the boundary scales according to

$$H^2 \sim \frac{Q^3}{8\pi^3 g \nu R^4}. \tag{2.3}$$

Defining the characteristic height

$$H^* = \sqrt{Q^3/(8\pi^3 g \nu R^4)}, \tag{2.4}$$

the expression for $h_{\text{crit}}$ reduces to

$$h_{\text{crit}} = \gamma H^*, \tag{2.5}$$

with a dimensionless scaling constant $\gamma$. The value of the scaling constant was determined in experiment described below.

### 2.2. *Experiments*

To accurately measure the transition depth, a reliable way of controlling the position of the disk relative to the water surface is needed. This was achieved by attaching the disk's bottom to a nut, which could move on a vertical threaded rod fixed to the vessel's bottom, as shown in Figure 2a. Turning the disk by $10°$ raised or lowered the disk by $54\mu$m, providing a vertical travel of 8 mm.

The jet originated from water directed through a straight vertical pipe, 1 meter in length. This allowed for flow laminarisation and produced a smooth jet impacting the disk. Water flow ($Q$) was regulated by a valve and quantified using a flow meter. The width of the jet was varied by changing the nozzle radius or the distance between the nozzle and the disk. The jet's radius was experimentally determined by photographing the jet from the side. After enhancing the contrast of the photo, computer image analysis was employed to identify the jet's edges and subsequently measure its radius. This process is illustrated in Figure 2b. For each measurement, 5 photos were taken, and the results were averaged. The mean value had an estimated uncertainty of 1%. Knowing the water flow and jet radius ($r$), the cross sectionally averaged velocity of the jet was found using relation:

$$Q = \pi r^2 U. \tag{2.6}$$

The experiment is sensitive to the downstream boundary condition (cf. for example Bush *et al.* (2006)). We utilised a large cylindrical vessel, measuring 31 cm in height and 50 cm in diameter, which was carefully levelled. This ensured minimal water height deviations at the container's edge (less than 3 mm). It was difficult to achieve better accuracy due to surface tension effects at the edge of the container. As water was overflowing the edge of the vessel, the submersion depth of the disk remained constant during the experiment.

The setup was used to determine the submersion depth of the disk at which the type I and type IIa jumps occurred across various values of $Q$ and $U$. Each series was executed while maintaining a constant nozzle height above the water (note that $U$ was variable in these series). The transition between different jump types did not occur simultaneously across the entire disk. Instead, during these transitions, we observed a type I jump on some parts of the disk and a type IIa jump on others. For each measurement, we recorded the greatest depth for which type I jump was pronounced and the shallowest depth for which type IIa jump was pronounced. The experimentally measured critical height, denoted as $h_{\text{crit}}$, was calculated as the average of these extreme values. An illustrative measurement series for jump height is depicted in Figure 3a. Utilising the presented scaling analysis (2.5), we were able to combine all measurement series into a single master curve, as shown in Figure 3b.

Within the studied parameter range, the critical height $h_{\text{crit}}$ adheres to the predicted linear relationship (2.5). A deviation from linear dependency can be noticed for $h_{\text{crit}} \lesssim 2.5$ mm which aligns with the capillary length of water $l_{\text{cap}} \approx 2.7$ mm. This implies that surface tension phenomena might influence the value of $h_{\text{crit}}$ at smaller $H^*$ values.

## 3. Unsinkable disk

The phenomenon, referred to as the *unsinkable disk*, emerges when a vertically directed jet impinges upon the centre of a freely floating metallic disk. Under specific conditions, a disk that would ordinarily submerge can instead achieve a floating equilibrium. Remarkably, this phenomenon exhibits self-stabilising characteristics; when the disk is disturbed, either by a change in inclination or position, it returns to a stable configuration.

   Initial observations revealed that the phenomenon of the unsinkable disk manifests exclusively under type I jump conditions. Conversely, the disk sinks when a type IIa jump is observed. This insight suggests that the system parameters needed for the disk to float are congruent with those that give rise to a type I jump. This correlation can be intuitively understood. In the case of a type IIa jump, a water vortex forms— as depicted in Figure 1c — which redirects the water back onto the disk. This change diminishes the effective buoyant force, ultimately causing the disk to sink.

### 3.1. *Force balance*

For the disk to achieve a state of equilibrium, in which it floats, the net force exerted upon it must be zero,

$$0 = F_b - F_j - F_g. \tag{3.1}$$

The forces contributing to this equilibrium include: the force generated by the impinging jet, $F_j$; the gravitational force acting on the disk, $F_g$; and the hydrostatic pressure exerted on the disk's underside, which manifests as an upward buoyancy force $F_b$. The force exerted by the water jet with radius $r$ and flux $Q$ can be expressed as (Stephens & Ward 1972)

$$F_j = \rho \frac{Q^2}{\pi r^2}. \tag{3.2}$$

The buoyant force acting on the disk can be decomposed into two distinct components: the first component arises from the buoyancy attributable to the volume $V$ displaced by the disk itself; the second component depends on the volume of air located above the disk, which, due to negligible thickness of the water layer, is a function of the disk's floating depth $h_{float}$ and its surface area $S = \pi R^2$:

$$F_b = \rho g (V + h_{float} S). \tag{3.3}$$

Utilising equations (3.2) and (3.3), and by introducing the effective mass of the disk as $m_{eff} = m_{disk} - \rho V$, the floating depth can be formulated as a function of the relevant parameters:

$$h_{float} = \frac{m_{eff}}{\rho S} + \frac{Q^2}{g S \pi r^2}. \tag{3.4}$$

The depth at which the disk floats shows a quadratic increase in response to the rising water flux ($Q$). On the other hand, the disk can only float if the jet has enough momentum to displace the necessary amount of water. Following the observation that the disk floats only when type I jump occurs $h_{float} < h_{crit}$, a condition for the disk to float is found:

$$\gamma \sqrt{\frac{\rho^2 Q^3 g}{8\pi \nu}} < g m_{eff} + \rho Q U \tag{3.5}$$

which establishes a relationship between the water flux ($Q$) and the jet velocity ($U$), required for achieving disk flotation. In our theoretical calculations we used density of water $\rho = 997 \, \text{kg/m}^3$, and its kinematic viscosity $\nu = 10^{-6} \, \text{m}^2/\text{s}$ as reported by Cooper & Dooley (2008).
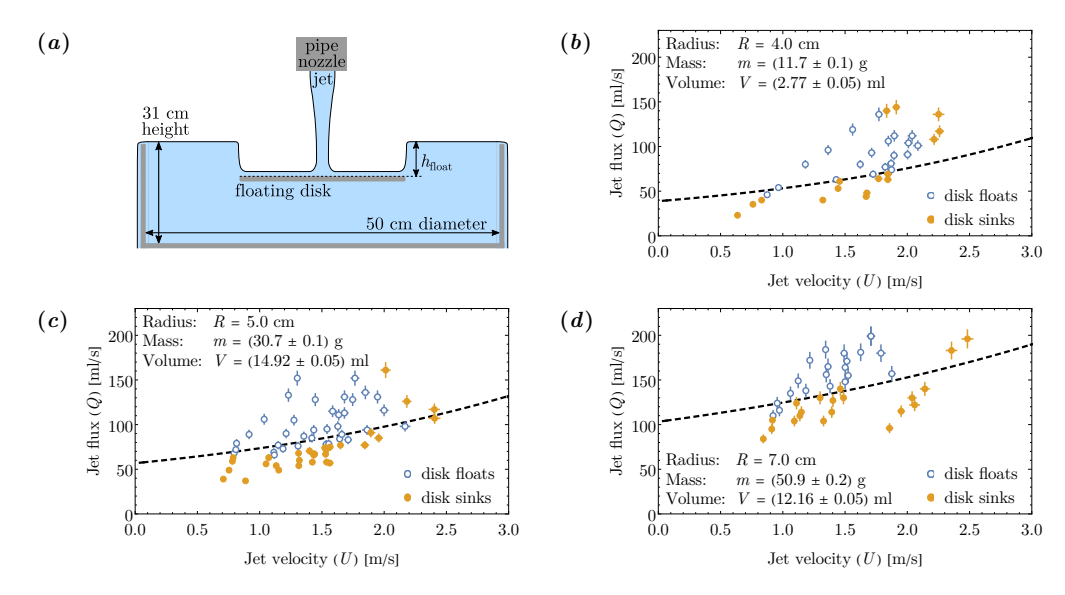
Figure 4: The diagram (a) illustrates the experimental setup used to investigate whether the disk would float or sink. The flow rate $Q$ and the jet radius $r$ were independently manipulated by changing the diameter of source pipe and adjusting the distance of the nozzle from the water surface. $Q$ and $r$ were used to compute the jet velocity $U$. The results (b-d) from the floating/sinking measurement experiments, alongside the theoretical prediction of the float/sink boundary (indicated by the dashed black line) show good quantitative agreement. The parameters of the disks used in these experiments are summarised in the charts.

### 3.2. *Experiments*

To test the necessary conditions for the disk to float, a similar experimental setup to the one described in the Section 2.2 was used. This time, the disk was unrestricted and free to move in all directions, as shown in Figure 4a. The disks used in the experiment were carefully positioned beneath the jet and subsequently released. We observed that the disks sank almost immediately when the jet flux $Q$ and the jet velocity $U$ were insufficient. The disk was considered to be floating if it remained on the surface for at least 15 seconds.

The disks used in the experiments were approximately 0.1 mm thick and made of aluminium. To adjust the weight of the disks, and to overcome the effects of the surface tension, copper washers were glued to their underside. The additional buoyancy and weight resulting from these modifications have been taken into account in the comparison with theoretical predictions.

We studied $U$ in range from 0.6 m/s to 2.5 m/s and focused specifically on values of the water flux $Q$, that are close to the threshold between the states of floating and sinking. Measured behaviour of the disks, along with the theoretically predicted float/sink boundary, are depicted in Figure 4b-d. We noticed that when values of flux $Q$ were sufficiently high the disk would remain afloat. Conversely, when the values of $Q$ were too low, the disk would gradually sink by increasing its floating depth. This process continued until the hydraulic jump collapsed, allowing water to flow onto the disk.

The theoretical model generally aligns well with most of the cases studied. However, deviations from the theoretical predictions were observed for higher values of $U$. In these instances, despite the theory suggesting that the disk should remain afloat, it sank during our experiments. In these instances, the disk exhibited oscillations of increasing amplitude,

characterised by lateral movement and tilting, where the jet notably forced the impacted segment of the disk downward. At a certain point, the tilt became so pronounced, and the submersion of the disk's lower side so deep, that the water jump could no longer prevent ambient water from overflowing onto the disk, leading to its eventual sinking.

While the analysis of disk rotational stability falls outside the scope of this paper, it is worth noting that in the instances where the disk was floating, any slight disturbance in its position relative to the jet resulted in a consistent return to its stable position. Interestingly, our static theoretical analysis predicted floating even in cases of oscillatory sinking. This discrepancy highlights the necessity of incorporating disk dynamics into considerations for a comprehensive understanding of this phenomenon.

## 4. Conclusions

Our study demonstrates that directing a vertical jet onto a disk from above can prevent the disk from sinking. This effect is attributed to the phenomenon of the parametric hydraulic jump, which displaces water from the top of the disk, thereby generating an additional upward buoyancy force. We identified two distinct types of hydraulic jumps, type I and IIa, and established that maintaining the disk's flotation is feasible under type I jump conditions.

The parametric hydraulic jump differs from classical consideration, as the position of the water jump is fixed by the geometry of the setup. In this specific case, we utilised a scaling law to determine the critical submersion depth at which the transition from type I to type IIa jump occurs. The scaling constant of the model, $\gamma = 0.624 \pm 0.010$, was determined in an independent experiment aimed at measuring the submersion depth corresponding to this critical transition between jump types.

The phenomenon was studied experimentally across a broad range of parameters, including disk's radius, jet's flux, and jet's radius. Results were compared against the theoretical model, demonstrating substantial agreement in nearly all the cases examined. Notably, at high values of the jet flux and velocity, the disk displayed signs of instability, characterised by progressively intensifying oscillations. This observation indicates that while the proposed model establishes necessary conditions for disk flotation, it does not yet encompass all the sufficient conditions required for a comprehensive understanding of the phenomenon.

REFERENCES

Baayoun, A., Khayat, R. E. & Wang, Y. 2022 The transient spread of a circular liquid jet and hydraulic jump formation. *J. Fluid. Mech.* **947**, A34.

Bhagat, R. K., Jha, N. K., Linden, P. F. & Wilson, D. I. 2018 On the origin of the circular hydraulic jump in a thin liquid film. *J. Fluid. Mech.* **851**, R5.

Bohr, T., Dimon, P. & Putkaradze, V. 1993 Shallow-water approach to the circular hydraulic jump. *J. Fluid. Mech.* **254**, 635–648.

Bohr, T. & Scheichl, B. 2021 Surface tension and energy conservation in a moving fluid. *Phys. Rev. Fluids* **6**, L052001.

Bush, J. W. M., Aristoff, J. M. & Hosoi, A. E. 2006 An experimental investigation of the stability of the circular hydraulic jump. *J. Fluid. Mech.* **558**, 33–52.

Cooper, J. & Dooley, R. 2008 International association for the properties of water and steam: Release on the iapws formulation 2008 for the viscosity of ordinary water substance. *IAPWS Release, IAPWS Secretariat* .

Duchesne, A., Andersen, A. & Bohr, T. 2019 Surface tension and the origin of the circular hydraulic jump in a thin liquid film. *Phys. Rev. Fluids* **4**, 084001.

Duchesne, A. & Limat, L. 2022 Circular hydraulic jumps: where does surface tension matter? *J. Fluid. Mech.* **937**, R2.

Ellegaard, C., Hansen, A. E., Haaning, A. & Bohr, T. 1996 Experimental results on flow separation and transitions in the circular hydraulic jump. *Phys. Scr.* **1996** (T67), 105.

Ivanova, K. A. & Gavrilyuk, S. L. 2019 Structure of the hydraulic jump in convergent radial flows. *J. Fluid. Mech.* **860**, 441–464.

Landau, L. D. & Lifshitz, E. M. 1987 *Fluid Mechanics, Second Edition: Volume 6 (Course of Theoretical Physics)*, 2nd edn. *Course of theoretical physics, Vol. 6* 2. Butterworth-Heinemann.

Rayleigh, L. 1914 On the theory of long waves and bores. *Proc. R. Soc. Lond.* **90** (619), 324–328.

Stephens, R. C. & Ward, J. J. 1972 *Applied Mechanics*. London: Macmillan Education UK.

Teymourtash, A. R. & Mokhlesi, M. 2015 Experimental investigation of stationary and rotational structures in non-circular hydraulic jumps. *J. Fluid. Mech.* **762**, 344–360.

Wang, Y. & Khayat, R. E. 2018 Impinging jet flow and hydraulic jump on a rotating disk. *J. Fluid. Mech.* **839**, 525–560.

Wang, Y. & Khayat, R. E. 2019 The role of gravity in the prediction of the circular hydraulic jump radius for high-viscosity liquids. *J. Fluid. Mech.* **862**, 128–161.

Watson, E. J. 1964 The radial spread of a liquid jet over a horizontal plane. *J. Fluid. Mech.* **20** (3), 481–499.

Yokoi, K. & Xiao, F. 1999 A numerical study of the transition in the circular hydraulic jump. *Phys. Lett. A* **257** (3), 153–157.